

# Climate change impacts on water resources – studies in Japan

**Toshiharu Kojiri**

Water Resources Research Center, DPRI, Kyoto University, Kyoto 611-0011, Japan

**Climate change and global warming pose serious problems for sustainability of a sound human life. There have been many natural disasters such as floods, droughts, glacier collapses, typhoons, etc. Though many general circulation models have been developed and provided for worldwide hydrological and meteorological estimations, detailed causes and countermeasures on water-related disasters have not yet been resolved. Climate change and global warming in a river basin involve many different components such as hydrological, hydraulic and water resources viewpoints. Under these circumstances, water-related issues such as system dynamics, downscaling, river basin simulation and economic damage must be discussed to understand the impact evaluation linking it with human actions and the need for interdisciplinary collaborations.**

**Keywords:** Climate change, ecology, GCM outputs, hydraulics aspects, water resources utilization.

## Introduction

CLIMATE change and global warming pose serious problems for sustainability of a sound human life in the world. Many hydrological disasters such as floods, droughts, glacier collapses and typhoons have caused big and frequent damages to human lives and societies economically as well as physically. Though several general circulation models (GCMs) linked with ocean zones have been developed for downscaling river basins through regional climate models (RCM), the calculated resolution is not sufficiently satisfactory to determine the detailed causes and countermeasures. For flood control and water resources management, a spatial resolution of 1 km and a time scale of 1 h are required to describe the daily human and other living activities. Since climate change and global warming involve many different components for river basins from hydrological, hydraulic and water resource viewpoints. The IPCC<sup>1,2</sup> (Intergovernmental Panel on Climate Change) issued serious alerts against emission of greenhouse gases. This article focusses on the following issues to understand the impact evaluation under

those circumstances linking with interdisciplinary collaborations as shown in Figure 1.

Meteorological and hydrological aspects: (i) accuracy modification and downscaling of GCM outputs and (ii) water circulation in present and future conditions.

Hydraulic aspects: (i) probability of floods and droughts; (ii) landslide and debris flow; (iii) estimation of flood process for both inundation and inland waters; (iv) change of river channel and ecosystems; (v) water amenity change; and (vi) change of typhoon (hurricane) occurrence and storm surge.

Water resources: (i) feasibility and risk management of drought and water supply; (ii) estimation of cropping, vegetation, plantation and ecology changes; (iii) global water dynamics with trade, economics and natural source; and (v) new water utilization processes for agriculture, industry and human life.

## Socio-economic responses in large scale

### *Meta-information with regional water dynamics*

Worldwide economic linkages through trade, immigration, regional development and industry investment are related to both greenhouse gas emissions and countermeasure strategies against global warming. Since the present GCM outputs, whose resolutions are more than 200 km and 6 h provide worldwide hydrological and meteorological data under limited scenarios, the average global situation on water dynamics can be roughly estimated. To analyse the actual water circumstances such as floods and droughts, a downscaling approach with a resolution of 1 km and 1 h must be applied to the river basin<sup>3</sup>. To evaluate the impact results on human and social activities through water utilization processes, economic simulation in regional scale is significant to take the feedback of affected damage to water environment management as shown in Figure 2. GCM outputs, economic data and simulated results are handled as meta-information on a global scale. Setting these results as regional boundary conditions, a detailed river basin simulation is undertaken through downscaled GCM outputs.

In order to analyse many of Japan's water resources problems and related issues, it is necessary to consider the population and economic dynamics, and their influence

e-mail: tkojiri@wrcs.dpri.kyoto-u.ac.jp

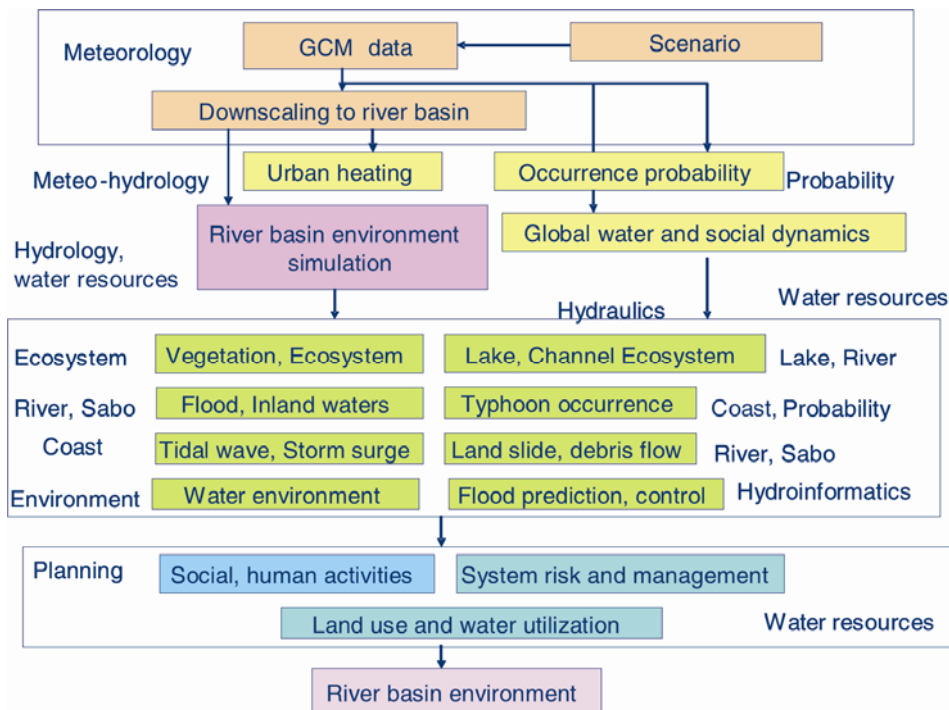


Figure 1. Relationship between water-related researches.

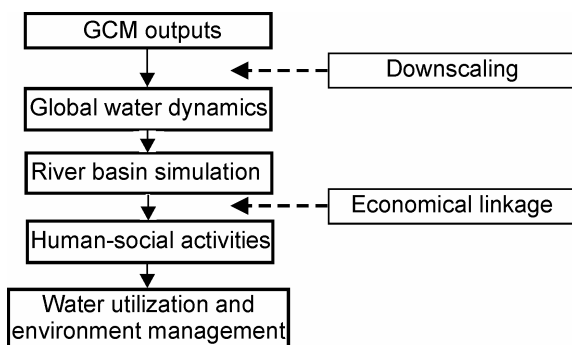


Figure 2. Relationship between GCM output and water environment management.

on water supply and demand, on a larger scale, taking into account the interactions between geographic regions. The island of Honshu, home to 80% of Japan’s population, is modelled in this study as a closed area. A system dynamics (SD) simulation can be performed to describe the changes in regional water resources distribution<sup>4,5</sup>. In this simulation, Honshu is divided into 10 regions: Tohoku-northwest, Tohoku-southeast, Kanto, Shinetsu, Hokuriku, Tokai, Chubu, Kinki, Sanin and Sanyo, with each region containing 11 sectors: population, land use, agriculture, industry, information technology, capital, pollution, water quality evaluation, water quality management, climate and water balance (see Figure 3).

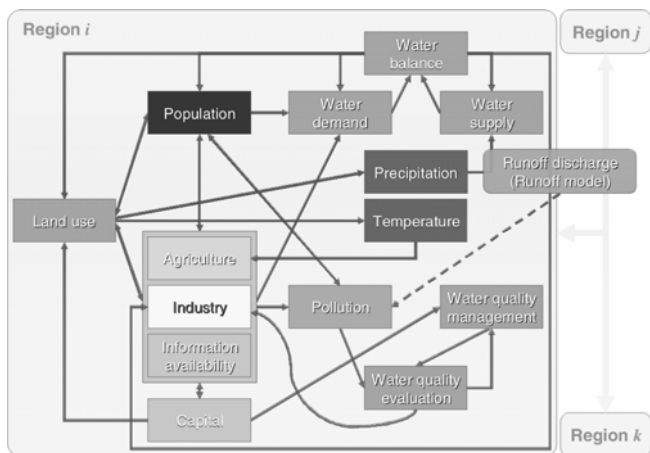


Figure 3. Schematic relationship of sectors in SD.

Formulation of sectors in system dynamics

A sector consists of some level equations and rate equations based on population, agriculture, industry and water balance. Population in each region is determined by birth, death, in-migrants and out-migrants. It is assumed that the death rate and the number of people determine the intraregional agricultural yields, industrial products and degree of pollutants at the river mouth as follows:

$$PL_r(k) = PL_r(j) + PR_{jkr} \cdot \Delta t, \tag{1}$$

$$PR_{jkr} = (PBR_{jkr} - PDR_{jkr}) + (PIMR_{jkr} - POMR_{jkr}), \tag{2}$$

$$POMR_{jkr} = POMAR_{jkr} + POMIR_{jkr} + POMXR_{jkr}, \quad (3)$$

where  $PL$  is the population in each region,  $PR$  the population growth rate,  $PBR$  the live births,  $PDR$  the deaths,  $PIMR$  the in-migrants,  $POMR$  the out-migrants,  $POMAR$  the out-migrants caused by agricultural yields,  $POMIR$  the out-migrants caused by industrial products and  $POMXR$  the out-migrants caused by water pollutants.

In the agricultural sector, for simplicity, only rice cropping is considered. Also, paddy fields require much more water than other agricultural fields. In the industrial sector, iron, chemical, and pulp and paper industries are considered as the main users of water resources. Water-recycling is also considered as recycled water plays a key role in these manufacturing processes. Agrochemicals from paddy fields and pollutant load from industrial and residential area, water-recycling, sewage treatment and self-purification processes are also considered. If the estimated water quality meets the effluent standard, water is discharged. However, if the effluent standard is not met, sewage treatment efficiency will come up, and a stricter effluent standard will be required for the industrial sector. The pollutant is formulated as follows:

$$XRL_r(k) = PL_r(k) \cdot UXR, \quad (4)$$

$$XERL_r(k) = XRL_r(k) \cdot STER_r, \quad (5)$$

$$XEAL_r(k) = XAL_r(k), \quad (6)$$

$$XEIL_r(k) = XIL_r(k) \cdot IWRR \cdot XCI \cdot STEI_r, \quad (7)$$

where  $XRL$  is the pollutant load from the residential area,  $UXR$  the pollutant load unit from residential area,  $UXD$  the pollutant load unit from domestic waste water,  $UXH$  the pollutant load unit from human waste,  $XERL$  the drained pollutant load from residential area,  $XEAL$  the concentration of drained agrochemical,  $XEIL$  the concentration of drained pollutant load from industrial area,  $STER$  the sewage treatment efficiency in residential area,  $STEI$  the sewage treatment efficiency in industrial area,  $IWRR$  the recycling rate of industrial water and  $XCI$  the progress of sewage treatment caused by request for stricter effluent standard. If demand for water is less than what is available, some measures concerning water resources will be taken up until the supply meets the demand.

The initial values of some levels and variables are determined and the levels calculated for every time unit. To modify the model, a 10-year-period from 1991 to 2000 is taken for verification. The calculation for the future is simulated until 2030. To understand the changing characteristics of water resources distribution, some scenarios are presented: namely creation of facilities for water supply, improvement of sewage treatment of industrial used

water, population decrease and global warming were assumed for calculation through location of industrial factories, comfortable residential area or cheaper workers. Figure 4 shows population change in central Japan. In this model, since people move from polluted water area to pure water area, death rate with bad quality must come up. Population in Kanto and Sanyo will rapidly decrease because people move to other regions. Figure 5 shows the change of industrial water demand due to the water demand which depends on economic situation in each area.

## GCM outputs in regional scales

### Downscaling of GCM outputs

Many studies have led to the development of GCMs to analyse impact assessments on global and regional scales. The newly developed model is called the coupled general circulation model (CGCM), linking the atmosphere and ocean. Since the resolution in CGCM output does not satisfy water resources researchers or planners, an effective downscaling approach is proposed to reduce the serious

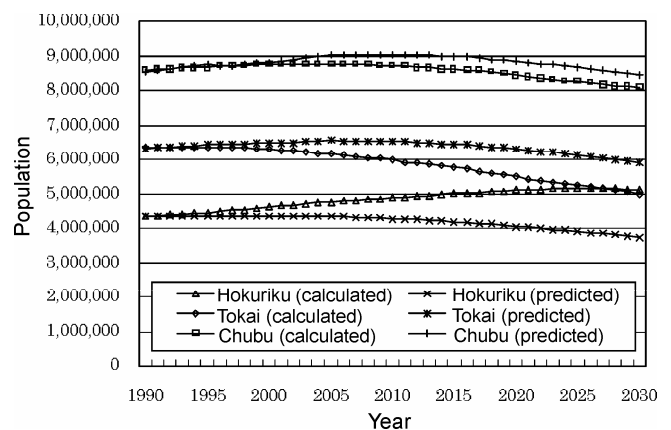


Figure 4. Population change (central Japan).

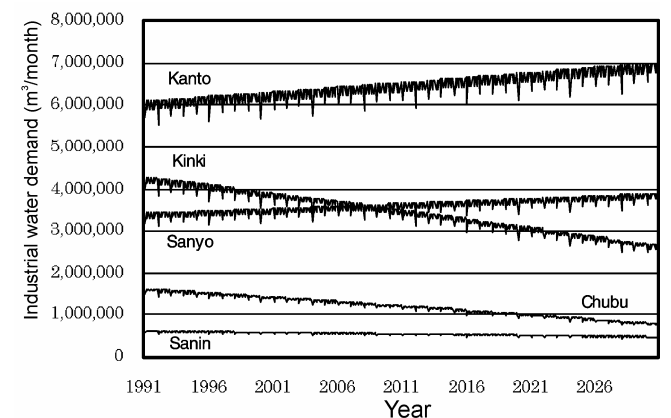


Figure 5. Change of industrial water demand.

gaps between CGCM and water resources management on a regional scale.

An hourly rainfall pattern with multi-observation points is generated with the modified weather generator for the classified meteorological patterns on a regional scale. A two-step approach is proposed<sup>3</sup>. First, the conditional rainfall probability is calculated every six hours through statistical data. Setting  $Y(i, t) = 1$  for rainfall at cluster  $i$  and  $Y(i, t) = 0$  for no rainfall, the following probability is obtained:

$$p_m(0) = P \left\{ Y(i, t) = 1 \mid \sum_{k=1}^4 Y(i, t-k) = 0, t \in S_m \right\} \quad (8)$$

$$p_m(1) = P \left\{ Y(i, t) = 1 \mid \sum_{k=1}^4 Y(i, t-k) > 0, t \in S_m \right\}, \quad (9)$$

where  $p_m$  presents the rainfall probability for 24 h. With uniform random number  $\omega$ , the rainfall situation in the considered river basin is determined as follows:

$$\text{If } \sum Y(i, t-k) = 0, t \in S_m, Y(i, t) = 1 \text{ for } \omega \leq p_m(0), \quad (10)$$

$$\text{If } \sum Y(i, t-k) > 0, t \in S_m, Y(i, t) = 1 \text{ for } \omega \leq p_m(1). \quad (11)$$

The rainfall intensity is then estimated for the rainfall event. Midair data  $q_t$  of high correlation with rainfall is classified into the following three groups:

$$U(t) = \begin{bmatrix} 0, & q_t \leq m \\ 1, & m < q_t \leq m + 1.2s \\ 2, & m + 1.2s < q_t \end{bmatrix}. \quad (12)$$

Moreover, in each classified group, such probability density functions as gamma distribution for rainfall intensity are identified. Six-hour rainfall  $PRCP(t)$  in the whole river basin is generated with random number  $R_i$  in the following equation:

$$PRCP(t) = R_i. \quad (13)$$

*Runoff characteristics through river basin*

The distributed runoff model with downscaled data under the resolution of 1 km and 1 h unit was applied to the Gokase River located in the southern part of Japan<sup>6</sup>. The number of meshes was 977, and four directions and four layers system was introduced.  $\chi^2$  qualification for the applied gamma function in the weather generator satisfies the high significance of 5% risk.

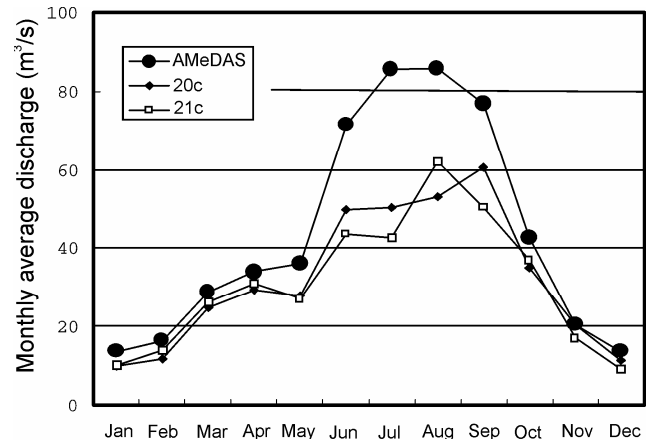


Figure 6. Discharge sequences after downscaling at the Gokase River.

Table 1. Relationship between precipitation and meteorological conditions at the Gokase River

Factor	Face height (hPa)	Correlation coefficient
Specific humidity	500	0.34
	850	0.49
Equivalent potential temperature	500	0.26
	850	0.44

The results simulated with observed data from 1971 to 2000 (the present re-calculation: 20th\_c experiment) underestimate the precipitation in summer due to less precipitation in June and July. On the other hand, for simulation with GCM outputs from 2071 to 2100 (the end of 21th century: 21th\_c experiment), 30–40% decrease in June and July, and 40% increase in August at the Gokase River basin. Totally, the hyetograph due to global warming will generate different feature patterns of the 20th century, especially in summer and winter. Figure 6 shows the downscaled results of the Gokase River discharge where the result of 20th\_c experiment underestimates the precipitation in summer because of lesser precipitation in June and July. In the warmer climate zone, the precipitation in June and July will decrease because no rainfall periods in the rainy season increase. Consequently, as discharge variation increases, natural disasters such as floods and droughts may occur more frequently. Table 1 denotes the special relationship between precipitation and meteorological conditions at the Gokase River.

**Water resources distributions in river basin scale**

*Integrated modelling of water circulation*

In the river basin, water quantity and quality are equally important for not only water utilization but also ecology

and water amenity. For water quantity, the heat balance method is introduced to calculate the evaporation and snowmelt at each mesh and each day. On the runoff process, the runoff model is applied with the kinematic wave method for surface and linear storage method for the first to fourth layer of groundwater.

For water quality, the water temperature and water pollutant are analysed from an environmental viewpoint. Assuming that soil temperature at the bottom of layer  $D$  is constant according to the annual atmosphere temperature, the soil temperature at  $y(m)$  depth from surface is formulated as follows:

$$\theta_g(y,t) = \theta_0 + D e^{-y\sqrt{\pi/\chi T}} \sin\left(\frac{2\pi}{T}t - y\sqrt{\frac{\pi}{\chi T}}\right), \quad (14)$$

where  $\theta_0$  is the annual averaged soil temperature ( $^{\circ}\text{C}$ ),  $T$  the cycle (365 days),  $\chi$  the heat diffusion coefficient in the ground ( $0.04 \text{ m}^2/\text{d}$ ) and  $D$  the amplitude of the surface temperature of soil. The ground water temperature is equal to the soil temperature and the water temperature released from sewerage is also equal to the atmosphere temperature because of negligible influence of runoff process on the urbanized sewerage. The water temperature in paddy field is calculated through the heat balance method among precipitation, atmosphere and river in the case of irrigation season<sup>7</sup>. The water temperature in river is represented by the following differential equation:

$$C\rho DY\left(\frac{\partial\theta_{\text{riv}}}{\partial\theta}\right) = H_0 + \frac{C\rho}{AW} \sum_v q_{\text{Iv}}(\theta_{\text{Iv}} - \theta_{\text{riv}}), \quad (15)$$

where  $C\rho$  is the specific heat at constant pressure ( $\text{cal/g}^{\circ}\text{C}$ ),  $\rho$  the atmosphere density ( $1.0 \times 10^6 \text{ g/m}^3$ ),  $DY$  the mean water depth (m),  $\theta_{\text{riv}}$  the temperature of channel water ( $^{\circ}\text{C}$ ),  $H_0$  the heat balance per unit square ( $\text{cal/m}^2/\text{s}$ ),  $AW$  the surface area ( $\text{m}^2$ ),  $q_{\text{Iv}}$  the inflow from element  $v$  ( $\text{m}^3/\text{s}$ ) and  $\theta_{\text{Iv}}$  the inflow temperature.

It is assumed that sewerage water from factories or houses flows down into the river through individual treatment tank, combined treatment tank or sewerage network for agriculture. The inflow concentration of waste water to the river is calculated according to pollutant load per unit activity as follows:

$$L_{\text{np}} = \sum L_{\text{np}u} A_u / A, \quad (16)$$

where  $L_{\text{np}u}$  is the released load unit of non-point pollutant for land use  $u$  ( $\text{mg/m}^2/\text{day}$ ), and  $A_u$  the area of land use  $u$  ( $\text{m}^2$ ). The traction load of piled material from non-point source is represented in proportion to the square of runoff height as follows:

$$L_{\text{swp}} = k_{\text{wnp}} P_{\text{np}} Q_h^2 A, \quad (17)$$

where  $Q_h$  is the horizontal runoff height (m/h),  $k_{\text{wnp}}$  the traction coefficient due to non-point source ( $\text{h/m}^2$ ), and  $P_{\text{np}}$  the piled pollutant load ( $\text{mg/m}^2$ ).

To verify the proposed methodologies, the upper Shonai River, which is about  $500 \text{ km}^2$  area and located in the centre of Japan, is applied for the observed data of 1994. Figure 7 shows the simulated results under conditions of assumed climate changes that are set at temperature rise of  $2^{\circ}\text{C}$  and no change of other factors such as precipitation, sunshine, released water temperature from houses and so on. The increase of surface temperature is relatively small besides  $4^{\circ}\text{C}$  increase in August due to long wave radiation. The precipitation temperature equal to the atmosphere near surface shows a stable increase for whole periods. On the contrary, the water temperature in paddy field goes down because the increase of latent flux is greater than other fluxes. Though a significant reduction of river water temperature occurs during the irrigation time, the averaged change seems to be less than the temperature change.

#### Evaluation of water environment through endocrine disruptor

Endocrine disruptors are widely recognized in many river basins in Japan as undesirable factors which cause serious damage to ecosystem. Nonylphenol is frequently detected as one of the controlled factors in rivers. To evaluate environment quality, the population of aquatic creatures (fish) is employed as the impact on ecology because fish is classified as one of the typical species affected by water quality. Physiology-based pharmacokinetic model (PBPK) is introduced to simulate the affected processes as compartment model such as taking up of the dissolved chemicals into the fish body through gill, taking process of the absorbed suspended materials as food and the

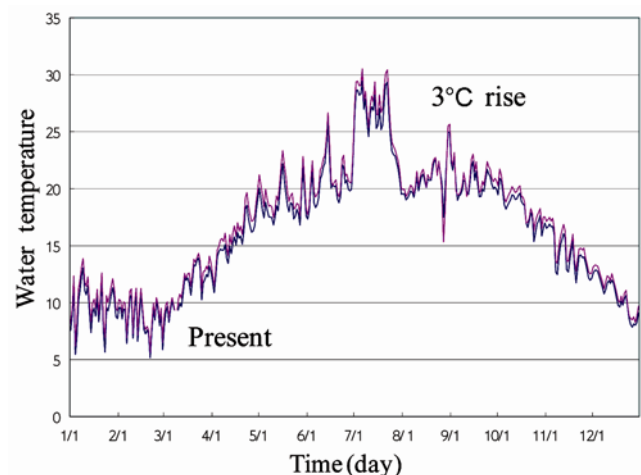


Figure 7. Impact analysis of climate change under the assumed scenarios.

chemical dynamics between the internal organs<sup>8</sup>. The chemical balance in the internal organs is represented as follows:

$$V_{organ} \frac{dM_{organ}}{dt} = G_{organ}^{in} (M_{organ}^{in} - M_{organ}) - \xi_{organ} M_{organ} V_{organ}, \quad (18)$$

where  $V_{organ}$  is capacity of the organ,  $M_{organ}$  the chemical concentration in the organ,  $G_{organ}^{in}$  the blood inflow into the organ,  $M_{organ}^{in}$  the chemical concentration in the organ, and  $\xi_{organ}$  the decomposition velocity for chemicals in the organ. Consequently, the population of fish is estimated using the logistic curve concept using the following equation:

$$\frac{dN_i}{dt} = \gamma N_i - \frac{\gamma}{\chi} N_i^2 - u(M_{organ}^i - M_{organ}^{i,threshold}) N_i, \quad (19)$$

where  $N_i$  is total population of considered aquatic creature at growth level  $i$ ,  $\gamma$  the natural increase rate of population,  $\chi$  the environmental capacity,  $u$  the coefficient of extinction velocity, and  $M_{organ}^{i,threshold}$  the threshold value. The environment index is defined as integration of all impacts according to the growth levels of the biota. The impact of population change with and without chemical exposure is represented as follows:

$$R_i = N_i^{with} / N_i^{without}. \quad (20)$$

$N_i^{with}$  is the population of aquatic creatures exposed to chemicals at growth level  $i$  and  $N_i^{without}$  is the population of creatures without exposure to chemicals. The recreation potential of population can then be calculated as follows:

$$\Delta R = \prod R_i, \quad (21)$$

where  $R_i$  is population level impact in each life stage  $i$ . The given parameters are presently not sufficient to show all ecological conditions because their values are decided not through eco-toxicology but their ichthyological aspect<sup>9</sup>.

**Table 2.** Estimated reproductive potential on the next generation at reference points

	Adult	Juvenile	Egg	Reproductive potential (%)
Ena	92.4276	24.2763	100	22.438
Yamaoka	99.867	98.6699	100	98.5387
Toki	99.9389	99.3887	100	99.328
Shidami	99.996	99.9958	100	99.9918

Table 2 shows the estimated impact of nonylphenol concentrations and reproductive potentials on the next generation of the assumed aquatic biota. As the adult fish will have higher concentration of nonylphenol in its liver than the juveniles, its chances of survival are lower due to higher impact of exposure to toxic chemicals. The egg is not greatly affected because of hard shell and no adaption. Though the averaged impact index of chemical exposure on fish yields only 1% decrease of population in downstream area, the maximum impact results in more than 75% decrease.

### Impacts assessment of climate change in river basin scale

#### Hydrological characteristics

The impacts of global warming on water resources and ecosystem in the whole river basin running the distributed hydrological and environmental model simulation with GCM outputs are assessed for the periods ‘1979–2000’ and ‘2079–2100’ to estimate future serious circumstances and necessary countermeasures. Figure 8 shows the inter-relationship between hydrology and water resources events affected with global warming and urbanization. Flood and drought controls with reservoir operation should be updated considering future water quantity and quality sequences. Meteorological changes cause suitability changes of ecological characteristics such as habitat area and species, and vegetation. Urbanization and deforestation cause additional damages to geological conditions through soil erosion and removing, and flood/drought risk for water retention potential.

Since evapotranspiration in the Thornthwaite method has a strong relationship with air temperature, the same patterns for the present and future results in average monthly differences of 0.5 mm under air temperature rise of 5°C in the Nagara River basin. The annual increase is approximated with 100 mm. Through simulation, the starting periods of snowfall between the two cases are in the

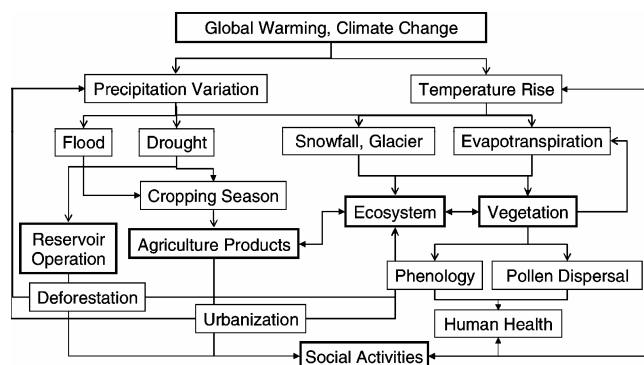


**Figure 8.** Evaluation flow due to climate change.

same month (November), and the disappearance period (May) from 2079 to 2100 comes one month later (June) from 1979 to 2000 in the catchment average. Through spatial distributions of snowfall, it is clear that snow depth is apparently affected by temperature rise. The volume of snowfall may be half the present situation. The annual discharge height through snowmelt decreases to 150 mm due to high temperatures. Water resources and snow will face serious situation not only in early spring but also in winter.

From June to September, these variations of averaged monthly discharge increase more than in other periods due to the rainy season. From the simulated water temperature sequence in the river collaborating with the spatial sequence in precipitation and discharge. From 2079 to 2100, water temperature rises by 1–3°C in the upper stream and declines in the lower stream because the surface and earth temperatures affect water temperature more than by water diffusion in the channel.

### Ecological change due to global warming

The assessed factors of ecological change are defined not only from hydrological viewpoint but also from ecological and living factors. Phenology is applied for zooid ecology, and the pollen dispersal and vegetation for vegetative ecology. Paddy (rice) and vegetables are considered for agricultural ones. The existence possibility of fish, recognized as a representative creature in water, is evaluated with water temperature and elevation without considering the water velocities and eddies in channel. Suitability is formulated with the fuzzy concept<sup>10</sup> as follows:

$$\ln_{\bar{i}} = T_i(x)G_i(x), \quad (22)$$

where  $\ln_{\bar{i}}$  is the suitability of sample family  $i$ ,  $T_i(x)$  the suitability against water temperature and  $G_i(x)$  the suitability against elevation.

On the simulated suitability for the considered aquatic creatures (fish), the fish that likes lower water temperature habitats are strongly affected by temperature rise and their inhabiting periods may also be shortened. The inhabiting suitability of sweetfish which like warm water seems small with wide variation in summer. In spring and autumn, the inhabitable period becomes longer because the inhabiting suitability is improved with moderate water temperature.

Figure 9 shows simulated suitability for the considered aquatic creatures (fish). As water temperature changes vary in upper and lower channels, the living suitability is shifted to different directions and the inhabitable period may be shortened<sup>11</sup>.

Phenology is assessed by the flowering date of cherry blossoms. Cherry blossoms from 2079 to 2100 will bloom almost 10 days earlier than at present. On suita-

bilities for laurel and deciduous forests in warm temperature zones, though laurel forest does not present simulation difference between 1979–2000 and 2079–2100, deciduous forest suitability was smaller because the proper area for deciduous forests decreased by 20% to 30%. On the other hand, subtropical forest suitability will occupy a wider area in most catchments because the suitability gets a value of 1. Through spatial distribution from 2079 to 2100, the suitable zone for deciduous forests may move to a more suitable one of subtropical evergreen forests due to the changeable suitability map. In specified areas, pollen scattering is not found because dormancy break does not happen.

The rice cultivation period gets extended while comparing the simulated results of the present and forecasted conditions. The harvesting date may arrive about 10 days earlier than the present because the accumulated temperature is higher. The water temperature suitability of the forecast period is lower than the re-simulated result in the nourishment of the initial farming and final growing seasons. Rice seems to have high sustainability against the lower suitability (0–0.5) of cool water at 11°C. The total impact assessment due to global warming on the Nagara River in Japan is summarized in Table 3.

### Economic damage of drought event in river basin

#### Estimation of water demands

Economic and physical damages due to climate change should be discussed as serious impacts on human life.

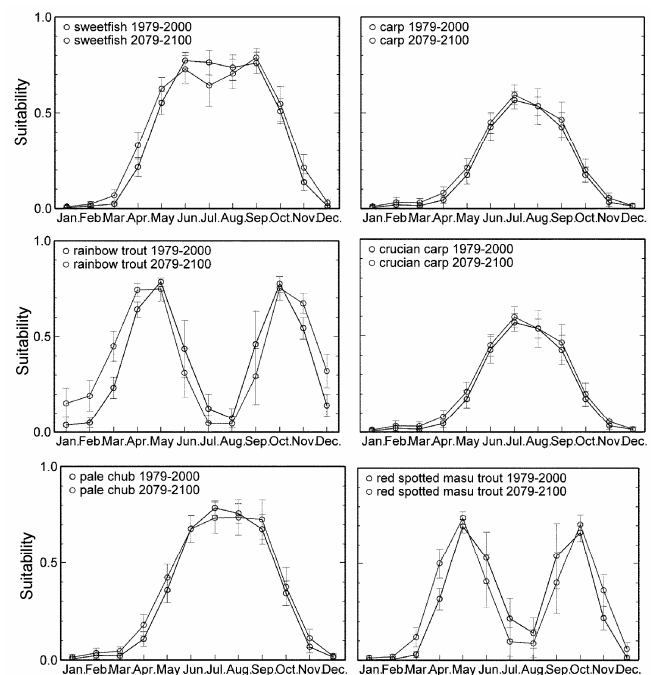


Figure 9. Monthly inhabiting suitability sequences.

**Table 3.** Summary of hydrological and environmental impacts in the Nagara River basin

Evaluation item	Main changes	Changes and effects
Temperature	Rise	ES
Precipitation	Increase/increase deviation	ES
Evapotranspiration	Increase	ES
Snowfall–snowmelt	Decrease/period shortening	ES
Discharge, runoff	Increase/increase deviation	ES
Water temperature	Rise	ES
Ecosystem (fish)	Suitability change/no change	ES/SH
Phenology	Timing change	ES/PW
Vegetation	Suitability change/no change	PW
Pollen	Timing change	ES/PW
Agriculture	Suitability change/timing change	ES/PW

ES: expansively or strongly influenced, PW: partly or weekly influenced, SH: sparsely or hardly influenced.

**Table 4.** Applied scenarios for global warming

	$\Delta T^{\circ}C$	$\Delta P$
Case 1	$\pm 0$	$\pm 0$
Case 2	+	$\pm 0$
Case 3	+	+10
Case 4	+	-10

The evaluation method for drought event can be transferred to water shortage. In the real world, the necessary water demands for agriculture, industry and municipal activities are estimated under the functions of temperature, precipitation, and previous intake discharge volume as follows.

**Agriculture**

$$QA(t+1) = -0.03 - 0.01R(t-4) + 0.02T(t-4) + 0.83QA(t) + 0.14QA(t-2); \tag{23}$$

**Factory**

$$QF(t+1) = 0.10 + 0.67QF(t) - 0.10QF(t-1) + 0.10QF(t-2) + 0.14QF(t-3); \tag{24}$$

**Municipal**

$$QC(t+1) = 0.20 + 0.01T(t-4) + 0.63QC(t) + 0.09QC(t-1) + 0.09QC(t-2); \tag{25}$$

where  $QA(t)$  is intake water for agriculture at time  $t$ ,  $QF(t)$  the water intake for factory (industry),  $QC(t)$  the water intake for municipal activities,  $R(t)$  the precipitation and  $T(t)$  the temperature for simulation.

The following scenarios are introduced as designated scenarios (Table 4):

- (i) same CO<sub>2</sub> emission is maintained for all periods;
- (ii) in other case, CO<sub>2</sub> increase is assumed with constant increase rate;

- (iii) temperature rise is set as  $\Delta T = 3^{\circ}C$  on a global scale;
- (iv) the land use situations are not changed with same runoff parameters; and
- (vi) precipitation is set as three variations of  $\Delta P = (-10.0\%, 0.0\%, +10.0\%)$  though the precipitation increase in global scale may be evaluated as +2–9%.

The average precipitation is changed according to temperature rise and the standard deviation is obeyed with constant variability rule. In the case of temperature rise (case 2), non-precipitation periods become shorter and continuous precipitation periods stay longer. As for the annual precipitation, the specified area should get more precipitation than average due to higher evapotranspiration in the area, the additional precipitation increase must be reasonable. The additional precipitation rate is allowed up to 4.5% against 10% increase and 3.6% against -10% increase cases.

*Economic damages*

The equivalent variation approach<sup>12</sup> is introduced to evaluate the economical drought damage in the river basin. Drought probability is assumed to be changed from  $P$  to  $P'$  due to global warming. Then, the utility level should be changed from  $E[U_p(I)]$  to  $E[U_{p'}(I)]$ . The house or society should bear with this difference between utilities of  $E[U_p(I)]$  and  $E[U_{p'}(I)]$  under the future global warming, the difference can be recognized as the inevitable damage. Case 3 will not estimate the serious damage because of less drought probability.

$$E[U_p(I + EV)] = E[U_{p'}(I)], \tag{26}$$

where

$$E[U_p(I + EV)] = P \cdot U(I + EV, x, 1) + (1 - P) \cdot U(I + EV, x, 0) \tag{27}$$

$$E[U_{p'}(I)] = P' \cdot U(I, x, 1) + (1 - P') \cdot U(I, x, 0). \tag{28}$$

The parameters of CES type applied here are already identified in the same river basin as follows:

$$h \cdot E[U] = P \cdot [-(\rho/h) \{ \ln | W_1 x_1^{-\rho} + W_2 x_2^{-\rho} + W_3 (a_3 - x_3)^{-\rho} + W_4 (a_4 + x_4)^{-\rho} + W_5 (a_5 - x_5)^{-\rho} + W_6 (a_6 + x_6)^{-\rho} + W_7 (a_7 + x_7)^{-\rho} \} ] + (1 - P) \times [-(\rho/h) \{ \ln | W_1 x_1^{-\rho} + W_2 x_2^{-\rho} + W_3 (a_3 - x_3)^{-\rho} + W_4 (a_4 + x_4)^{-\rho} + W_5 (a_5 - x_5)^{-\rho} + W_6 (a_6 + x_6)^{-\rho} + W_7 (a_7 + x_7)^{-\rho} \} ], \tag{29}$$



**Table 5.** Estimated damage in the house

	Damage (1000 J-yen/house/y)	Damage (1000 J-yen/house/y)
Case 2.3.0	2.7	0.23
Case 3.3. +10	-8.4	-0.70
Case 4.3. -10	5.5	0.46

**Table 6.** Estimated damage at the river basin

	Damage (1,000,000 J-yen/y)
Case 2	490.8
Case 3	-1526.9
Case 4	999.8

where  $E[U]$  is the expected utility (10,000 J-yen),  $h$  the variance for identified error,  $W_i$  the weight for item  $i$ ,  $p$  the parameter for alternated item,  $x_1$  the monthly income (J-yen),  $x_2$  the house space ( $m^2$ ),  $x_3$  the commute time (min),  $x_4$  the sunshine hours per day (h),  $x_5$  the dairy shopping (min),  $x_6$  the public service (comfortable = 1), and  $x_7$  the risk for drought (drought = 1 or non-drought = 0). Assuming that  $P$  is the present drought probability and  $P'$  the simulated result, the following results are obtained.

As the drought probability increases on a small scale (Table 5), the damage does not present big impacts where, 2700 J-yen is for case 2 and 5500 J-yen for case 4 per house. Table 6 shows the whole damage to the river basin, the water resources planning and the utilization system against the serious drought caused by global warming, that should be employed in regional, river basin, national, and international levels.

## Conclusions

A long-term trend should be initiated to find the next feature pattern under the conditional transition process. The changing spatial land use patterns according to the social activities and economical development should be estimated through other methodologies. Economic damage is estimated using drought damage formula. In this article, the research programmes on (i) the water dynamics in large scale, (ii) the downscaling approach for GCM outputs, (iii) the river basin simulation and (iv) the estimation of economic damage carried out by Water Resources Research Center were introduced to get the following achievements:

(i) The water dynamics in Japan was formulated under the mathematical concept of SD and extended into the worldwide continental model.

(ii) The statistical downscaling was proposed combining the pattern classification for GCM outputs, and the

weather generator to calculate the runoff discharge through precipitation and temperature in 1 km and 1 h units.

(iii) On the river basin simulation, water quantity, quality and ecosystem can be handled on the same computer programming, in other words, platform with mesh-typed runoff model. The spatial and temporal changes of vegetations, aquatic creatures, agriculture products and phenology are assessed.

(iv) The economic damage is estimated through the concept of equivalent variation approach. The present drought situation is different from future global warming or climate change because the affected area and factors on global warming are wider and more complex even on a river basin scale than the temporary event of drought.

Finally, since the impacts of global warming and climate change are expanding in the world and can cause serious damage to both human life as well as earth, more innovative research can come up with significant countermeasures.

1. Intergovernmental Panel on Climate Change, Special Report on Emissions Scenarios, Cambridge University Press, 2000.
2. Intergovernmental Panel on Climate Change, Climate Change 2007: The Physical Science Basis, Cambridge University Press, 2007.
3. Kojiri, T., Kobayashi, T. and Nozawa, T., Estimation of precipitation variation in river basin scale with GCM outputs. 4th International Conference on Water Resources and Environment Research, 2008, pp. 1551-1562.
4. Forrester, J. W., *World Dynamics*, Wright-Allen Press, Cambridge, Massachusetts, 1971.
5. Kojiri, T., Hori, T., Nakatsuka, J. and Chong, T.-S., World continental modeling for water resources using system dynamics, XXX IAHR Congress, 2005.
6. Kojiri, T., Kinai, Y. and Park, J.-H., Integrated river basin environment assessment on water quantity and quality by considering utilization processes. Proceedings of the International Conference on Water Resources and Environment Research, 2002, vol. I, pp. 396-401.
7. Kondo, J., *Environmental Meteorology*, Asakura Publishing Company, 1994, pp. 1-333.
8. Nichols, J. W., Mckim, J. M., Andersen, M. E., Gargas, M. L., Clewell III, H. J. and Erickson, R. J., A physiologically based toxicokinetics model for the uptake and disposition of waterborne organic chemicals in fish. *Toxicol. Appl. Pharmacol.*, 1990, **106**, 433-447.
9. Braunbeck, T., *Fish Ecotoxicology*, Birkhauser Verlag, 1998.
10. Kojiri, T., Kuroda, Y. and Tokai, A., Basin simulation and spatial assessment on water quality and quantity with multi-layer mesh-typed run-off model. Proceedings of the International Conference on Large Scale Water Resources Development in Developing Countries, 1997, WQ1-WQ8.
11. Kojiri, T., Hamaguchi, T. and Ode, M., Assessment of global warming impacts on water resources and ecology of a river basin in Japan. *J. Hydro-Environ. Res.*, Science Direct, Elsevier, 2007, 164-175.
12. Morisugi, H. and Oshima, N., A method for evaluating household benefits of reduction in water-shortage frequency. *Proc. JSCE*, 1985, No. 359/IV-3, pp. 91-98.